

Published in final edited form as:

J Acquir Immune Defic Syndr. 2011 August 15; 57(5): 363–370. doi:10.1097/QAI.0b013e31821a603c.

Molecular Characterization of Stool Microbiota in HIV-Infected Subjects by Panbacterial and Order-Level 16S Ribosomal DNA (rDNA) Quantification and Correlations with Immune Activation

Collin L. Ellis^{1,4}, Zhong-Min Ma², Surinder K. Mann^{1,3}, Chin-Shang Li⁴, Jian Wu¹, Thomas H. Knight¹, Tammy Yotter¹, Timothy L. Hayes⁴, Archana H. Maniar¹, Paolo V. Troia-Cancio¹, Heather A Overman⁴, Natalie J. Torok¹, Anthony Albanese³, John C. Rutledge¹, Christopher J. Miller^{1,2}, Richard B. Pollard¹, and David M. Asmuth^{1,*}

¹University of California Davis Medical Center, Internal Medicine, Sacramento, CA

²California National Primate Research Center, Davis, CA

³Mather Veterans' Administration Hospital, Mather, CA

⁴University of California Davis, Davis, CA

Abstract

Background—The relationship between gut microbial community composition at the higher-taxonomic order-level and local and systemic immunologic abnormalities in HIV disease may provide insight into how bacterial translocation impacts HIV disease.

Methods—Antiretroviral (ART)-naive HIV patients underwent upper endoscopy before and nine months after starting ART. Duodenal tissue was paraffin-embedded for immunohistochemical analysis (IHC) and digested for FACS for T-cell subsets and immune activation (CD38+/HLA-DR+) enumeration. Stool samples were provided from patients and controls for comparison. Metagenomic microbial DNA was extracted from feces for optimized 16S ribosomal RNA gene (rDNA) real-time qPCR assays designed to quantify panbacterial loads and the relative abundances of proinflammatory Enterobacteriales order, and the dominant Bacteroidales and Clostridiales orders.

Results—Samples from 10 HIV-subjects prior to initiating, and from 6 subjects receiving, ART were available for analysis. There was a trend for a greater proportion of Enterobacteriales in HIV-positive subjects compared to controls ($p=0.099$). There were significant negative correlations between total bacterial load and duodenal CD4⁺ and CD8⁺ T-cell activation levels ($r=-0.74$, $p=0.004$ and $r=-0.67$, $p=0.013$, respectively). The proportions of Enterobacteriales and Bacteroidales were significantly correlated with duodenal CD4⁺ T-cell depletion and peripheral CD8⁺ T-cell activation, respectively.

***CORRESPONDING AUTHOR INFORMATION**, David M. Asmuth, M.D., Associate Professor of Medicine, Division of Infectious & Immunologic Diseases, Department of Internal Medicine, UC Davis, Medical Center, 4150 V Street, PSSB G500, Sacramento, CA 95817, (916) 734-8695 (office), (916) 734-7766 (fax), (916) 734-8532 (lab), david.asmuth@ucdmc.ucdavis.edu.

Publisher's Disclaimer: This is a PDF file of an unedited manuscript that has been accepted for publication. As a service to our customers we are providing this early version of the manuscript. The manuscript will undergo copyediting, typesetting, and review of the resulting proof before it is published in its final citable form. Please note that during the production process errors may be discovered which could affect the content, and all legal disclaimers that apply to the journal pertain.

These data were presented in part at the *American Gastroenterological Association (AGA) Institute section of Digestive Disease Week (DDW) 2010*: New Orleans Convention Center, New Orleans, LA, May 1–6th, 2010, at the *28th International AIDS Conference (IAC)*: Vienna, Austria, July 18–23, 2010; and at the IAS Pre-Conference Workshop: "Towards a Cure": HIV Reservoirs and Strategies to Control Them. Vienna, Austria 16–17 July, 2010

Clinical Trial Registry Number (Clinicaltrials.gov Identifier): NCT00870363; and NCT00661960.

Conclusions—These data represent the first report of quantitative molecular and cellular correlations between total/universal and order-level gut bacterial populations and GALT levels of immune activation in HIV-infected subjects. The correlations between lower overall 16S rDNA levels and tissue immune activation suggest that the gut microbiome may contribute to immune activation and influence HIV progression.

Keywords

HIV infection; 16S rDNA; gastrointestinal-associated lymphoid tissue; stool; duodenal tissue; peripheral blood mononuclear cells; CD8⁺ T-cell; CD4⁺ T-lymphocyte; microbes

INTRODUCTION

A hallmark of HIV disease is profound depletion of CD4 T-cells from gastrointestinal-associated lymphoid tissue (GALT) very early following primary infection.¹ During the acute phases of HIV/SIV infection, nearly all susceptible mature CD4⁺ lymphocytes are infected and presumably destroyed by viral infection.^{2, 3} It has been observed that T-lymphocyte depletion in the gastrointestinal tract leads to microbial translocation^{4, 5} and indeed, an important consequence of HIV-induced CD4⁺ lymphocyte depletion from GALT is believed to be gut microbial translocation as measured by blood concentrations of lipopolysaccharide (LPS), detection of universally-conserved microbial 16S ribosomal RNA gene sequences (rDNA) in plasma, and increased levels of peripheral blood CD8⁺ T-cell subsets with an activated phenotype.^{6, 7} Increased CD8⁺ T-cell activation was recognized as a key predictor of HIV disease progression very early in the epidemic, but the causes for these elevations remain uncertain.^{8, 9} Indeed, the very high levels of CD8⁺ T-cell activation decline with ART suppression of HIV plasma viral loads, but infrequently achieve the levels of HIV-negative controls. Thus, persistently elevated fractions of activated CD8⁺ T-cells despite suppressed HIV viremia suggest that multiple factors contribute to this abnormality.¹⁰ In addition, soluble CD14 (sCD14), a surrogate marker of monocyte activation, is believed to bind LPS in the serum and, in effect, neutralize the pro-inflammatory impact of LPS.¹¹ Similar to CD8⁺ T-cell activation, sCD14 levels correlate with HIV disease progression and death, and may represent a surrogate marker for bacterial translocation.^{12–14}

The influence of the gut microbiota composition on a variety of disease states has gained recent attention.¹⁵ The development of obesity, diabetes mellitus, and the metabolic syndrome may be related to a complex interaction of immune defects and nutritional/metabolic factors influencing the structure and function of gut microbial communities, which in turn initiate a cascade of local and systemic signaling pathways that contribute to the clinical condition.^{16–18}

Despite recent observations of the correlation between plasma bacterial pro-inflammatory antigens and HIV-associated immune activation, the potential relationships between gut microbiota composition at a higher-taxonomic level and HIV-associated systemic immunologic defects has not been explored using molecular quantitative techniques. While other investigators have focused on the impact of bacterial translocation on systemic immune activation in chronic HIV disease, we sought to first explore whether the bacterial populations in the intestinal lumen influence local and systemic immunologic parameters. We designed a set of pilot experiments to test the hypotheses that increased proportions of Enterobacteriales and Bacteroidales in the gut correlate with GALT CD4⁺ T-cell depletion and peripheral blood CD8⁺ T-cell activation in HIV patients. Enterobacteriales is a facultative-anaerobic taxon generally residing in human small bowel niches and Bacteroidales are quantitatively-dominant obligate-anaerobic taxa generally residing in

human large bowel niches. Both contain classically Gram-negative staining, proinflammatory/LPS containing pathogens that have been associated with disease in other settings.¹⁹

METHODS

Clinical design

Specimens from 12 HIV-infected subjects and 5 controls were used for this pilot project. All subjects signed an informed consent form approved by the UC Davis Institutional Review Board. Ten subjects underwent upper endoscopy for distal duodenal biopsy and stool collection prior to initiating ART and six had the same procedure performed after 9 months of ART. Only four of these six subjects had baseline stool samples available for longitudinal analysis.

Tissue and cellular analyses

Duodenal biopsies were either paraffin-embedded for immunohistochemical (IHC) analysis or underwent digestion to single-cell suspension for flow cytometry.²⁰ Peripheral blood mononuclear cells (PBMCs) were separated by Ficol-Hypaque and subsequently processed with the duodenal cells in identical fashion. Cells were stained with Aqua-viability dye and QuantumDot655 anti-CD45RA from Invitrogen, (Carlsbad, CA); PacBlue-anti-CD3 and FITC-anti-HLA-DR from Biolegend, (San Diego, CA); ECD-anti-CD4 from Beckman-Coulter (Brea, CA); and PE-anti-CD38, PE-Cy7-anti-CCR7 and APC-Cy5-anti-CD8 from Becton-Dickinson (San Jose, CA) according to manufacturers' recommendations. A custom Becton-Dickinson LSR II flow cytometer was used for data acquisition and analyzed with FlowJo (TreeStar, Ashland, OR). The analysis algorithm for a representative sample is demonstrated in Figure 1.

For IHC analysis, the primary antibodies were polyclonal anti-CD3 rabbit serum (Dako Inc., Carpinteria, CA) and monoclonal anti-CD4 mouse serum (Vector, Burlingame, CA). Binding of CD3 and CD4 receptors were detected simultaneously using Alexafluor 488-labeled polyclonal goat anti-rabbit IgG (Molecular Probes, Eugene, OR) and Alexafluor 568-labeled polyclonal goat anti-mouse IgG (Molecular Probes, Eugene, OR). The numbers of positive cells were counted by a single observer (Z-MM) and presented as cells/millimeter² of lamina propria of duodenal mucosa.^{21, 22} Representative sections are presented in Figure 2.

Stool DNA Extraction/Analysis—Meta-genomic microbial DNA was extracted by standard phenol-chloroform-ethanol-based methods from frozen stools as described by Hartman et al.²³ Molecular quantitation of bacterial 16S ribosomal-RNA genes (rDNA) was performed by kinetic (real-time) quantitative-PCR (qPCR). The oligo-primers used were previously optimized for evolutionarily-conserved total and order-level phylogenetic sequence-hybridization representative of human-gut Enterobacteriales, Bacteroidales, low-G +C Clostridiales, and panbacteria/total bacterial-load.²³

Primers (ATCC, Manassas, VA): Our chosen qPCR oligonucleotide primers have been confirmed for specificity and validity using the Ribosomal Database Project (RDP) probe-match website.²⁴

The panbacteria²⁵ (total bacterial load)

This Forward/Reverse (F/R) primer had a melting T (T_m) of 65.5°, an amplicon size of 180 base pairs (bp), a 16S position at 334–514, F/R coverage was 68/71%, a serially-diluted genomic standardization curve (note any bacterial species could have been used) with

Escherichia coli at 4.3×10^7 copies in 2 μ L nuclease-free water, an experimental water-control run in-parallel, and the following genomic sequences:

F primer ACTCCTACGGGAGGCAGCAGT; *R Primer* ATTACCGCGGCTGCTGGC.

The Bacteroidales order (class Bacteroidetes)²⁶ from the phylum Bacteroidetes

This F/R primer set had a T_m of 61°, an amplicon size of 151 bp, a 16S position at 1038–1189, F/R coverage of 56/59%, a serially-diluted genomic standardization curve with *Bacteroides fragilis* at 8.15×10^7 copies in 2 μ L nuclease-free water, an experimental water-control run in-parallel, and the following genomic sequences:

F Primer GGTGTCGGCTTAAGTGCCAT; *R Primer* CGGAYGTAAGGGCCGTGC.

The Clostridiales order (class Clostridia)²⁶ from the low-C+C phylum Firmicutes

This F/R primer set had a T_m of 60°, an amplicon size of 429 bp, a 16S position at 477–906, F/R coverage of 34/33% with subgroup F/R coverage of Lachnospiraceae of 76/65%, a serially-diluted genomic standardization curve with *Ruminococcus productus* at 4.4×10^7 copies in 2 μ L nuclease-free water, an experimental water-control run in-parallel, and the following genomic sequences:

F Primer CGGTACCTGACTAAGAAGC; *R Primer* AGTTTYATTCTTGCGAACG.

The Enterobacteriales order (class Gamma-Proteobacteria)²⁷ from the phylum Proteobacteria

This F/R primer had a T_m of 60.5°, an amplicon size of 177 bp, a 16S position at 1475–1652, F/R coverage of 59/34%, a serially-diluted genomic standardization curve with *Escherichia coli* at 4.3×10^7 copies in 2 μ L nuclease-free water, an experimental water-control run in-parallel, and the following genomic sequences:

F Primer ATGGCTGTCGTCAGCTCGT; *R Primer* CCTACTTCTTTTGCAACCCACTC.

Each qPCR-well was run in triplicates and contained 10 μ L of 2 \times Takara Perfect Real Time master mix (Takara Bio Inc., Otsu, Shiga, Japan) which included: 7.2 μ L of water, 0.8 μ L of a 10 μ M F/R primer mix, and 2 μ L of either an optimized dilution of 1:500 of extracted template DNA in nuclease-free water for specimen analysis or a serial dilution series of bacterial reference genomic DNA for standard curves. All reactions were paralleled by a non-template water control analysis (via the same nuclease-free water stock used for the other parallel reactions within the same experiment). Cycling conditions: 95 °C for 20 sec; 40 repeats of the following steps: 95 °C for 4 sec, 30 sec annealing. SYBR green fluorescence was detected with a BioRad Chromo4 Real Time PCR Detector on a Dyad Disciple Peltier Thermal Cycler (Bio-Rad Life Science Research, Hercules, CA). Melting curves were obtained from 55 °C to 90 °C, with fluorescence measurements taken at every 1 °C increase in temperature. Mean triplicate numbers of 16S amplicons/ μ L stool aliquot detected \geq log-fold above background noise-control were considered signal using MJ Opticon Monitor Analysis Software, Version 3.1 (Bio-Rad Life Science Research, Hercules, CA). Quality control parameters included amplification detection only at cycle10 or later, parallel slopes in log view, and an R^2 (correlation coefficient) value of 0.990 or higher.

Soluble CD14 Assay

Soluble CD14 levels in plasma samples were quantified by ELISA with the Quantikine Human sCD14 Immunoassay (R&D Systems, Minneapolis, Maryland, USA) according to the manufacturer's protocol. Samples were assayed in duplicate.

Statistical Methods

For the purposes of this pilot analysis, all subjects who were treatment-naïve (n=10) were compared to normal controls (n=5). Panbacterial quantities measured were used as denominators to calculate fractions or relative proportions of individual order-abundances. The two-sided Wilcoxon rank-sum test was used to compare the HIV-positive and control groups for numerical variables. The Spearman rank correlation coefficient was used to study the correlation between two quantitative variables. All analyses were performed with SAS v9.2 (SAS Institute Inc., Cary, NC, USA). All values were expressed as mean \pm standard deviation (SD) (median; minimum, maximum).

RESULTS

Baseline Clinical Data Results

Baseline data are available for all subjects (Table 1). Women and minorities are well represented in this cohort, constituting 42% and 33% of the total, respectively. Control subjects (n=5) were recruited from family and friends of clients in the HIV clinic who were of similar demographics. Mean \pm SD (median; minimum, maximum) pre-treatment plasma HIV load was 4.20 ± 0.64 (4.35; 2.99, 5.09) \log_{10} cp/mL for all subjects and all plasma HIV loads were undetectable at the time of the second biopsy, except for one who experienced an isolated blip to 251 cp/mL.

Gut tissue and blood analysis results

Mean \pm SD (median; minimum, maximum) duodenal CD3⁺/CD4⁺ percent was $5.9 \pm 3.2\%$ (6.0%; 1.9%, 10.1%) for pre-ART subjects and $13.1 \pm 6.8\%$ (9.1%; 7.9%, 22.3%) for post-ART subjects. The frequency of circulating CD8⁺ T-cells with an activated CD38⁺/HLA-DR⁺ phenotype was $50.9 \pm 12.5\%$ (53.1%; 30.8%, 63.4%) among the ART-naïve cohort and $29.8 \pm 9.4\%$ (28.5%; 18.8%, 42.0%) for ART-experienced subjects. In the duodenal tissue, the percent activated CD8⁺ and CD4⁺ T-cells was $60.6 \pm 7.1\%$ (61.6%; 48.4%, 68.9%) and $56.8 \pm 8.6\%$ (54.5%; 49.0%, 73.4%), respectively, among the ART-naïve cohort and $68.6 \pm 11.4\%$ (63.7%; 56.9%, 86.8%) and $54.7 \pm 10.1\%$ (53.8%; 44.3%, 67.2%) respectively, among the ART-experienced cohort. There was no difference in the duodenal tissue CD3⁺/CD4⁺ count in the pre-treatment versus on-therapy groups at 148.9 ± 44.2 (149; 81, 197) cell/mm² versus 153.5 ± 24.7 (155.5; 119, 185) cell/mm², respectively. These data suggest that the duodenal tissue lymphocyte compartment is not in equilibrium with peripheral blood immune reconstitution observed following HAART therapy, especially with respect to absolute CD4⁺ T-cell density and T-lymphocyte activation.

Group Differences in Bacterial Taxa

Total quantity of universal bacterial 16S rDNA and the relative proportion of bacterial orders in the stool are represented in Figure 3 panels A–D. Overall, the greatest quantity of panbacterial 16S rDNA was measured in the control population compared to the naïve HIV-positive population (5.5 ± 4.0 (4.6; 1.0, 10.4) versus 3.7 ± 3.2 (4.0; 0.00065, 10.5) [$\text{all} \times 10^8/\text{gram stool}$], respectively $p > 0.1$). There was a weak trend for a greater proportion of Enterobacteriales in HIV-positive patients compared to controls ($0.320 \pm 0.373\%$ (0.168%; 0.000086, 1.058%) vs. $0.038 \pm 0.047\%$ (0.015%; 0.0000186, 0.099%), $p=0.099$). There were no significant differences in the total quantity of universal 16S rDNA measured nor in the proportion of bacterial orders comparing the other cohorts or orders.

We next explored correlations between the stool bacterial populations and tissue/peripheral parameters of immunity (Figure 4 panels A–E). There was a negative correlation between the number of total/universal microbial 16S rDNA and the duodenal CD8⁺ and CD4⁺

activated T-cells in the ART-naïve cohort ($r=-0.67$, $p=0.013$ and $r=-0.74$, $p=0.004$, respectively) noting that the control subjects had the highest levels of 16S rDNA measured (Figures 4A and B). Higher fractions of Bacteroidales were significantly correlated with a higher percentage of CD8⁺ T-cells in PBMCs with the activated phenotype (Figure 4C). This relationship held whether subjects were grouped as treatment-naïve ($n=10$) or all sample points ($n=16$) ($p=0.019$ and 0.016 , respectively). Higher fractions of Enterobacteriales were significantly correlated with a low duodenal CD3⁺/CD4⁺ count by IHC regardless of whether subjects were grouped as treatment-naïve ($n=7$) or all sample points ($n=13$) ($p=0.023$ and 0.013 , respectively) (Figure 4D). Interestingly, the correlation between CD4⁺ T-cell counts in the duodenal tissue by IHC and the proportion of Enterobacteriales was strengthened when the samples from control subjects were included in the analysis ($r=-0.833$, $p=0.005$). No significant correlations were observed between Clostridiales order and tissue CD4⁺ T-cell count by IHC and CD8⁺ T-cell activation. Absolute peripheral CD4⁺ T-cell counts also did not correlate with any gut microbial quantitative measurements.

In order to explore whether the gut microbiota composition correlated with a surrogate marker for bacterial translocation *ad hoc*, plasma was available on a subset of subjects for sCD14 measurement ($n=13$). The sCD14 levels were 1.59 ± 0.40 $\mu\text{g/mL}$ (1.6; 0.84, 2.21). There was a weak negative correlation between total/universal microbial 16S rDNA and sCD14 levels ($r=-0.544$, $p=0.055$) (Fig 4E), which was similar to the correlations observed between total/universal microbial 16S rDNA and CD4⁺ and CD8⁺ T-cell activation in duodenal tissue. Interestingly, no correlations were observed between sCD14 levels and PBMC lymphocyte activation or individual microbiota orders. This suggests a possible intermediary, such as bacterial product translocation or cytokine cascade, as a primary consequence of total/universal microbial 16S levels in the gut of HIV-infected subjects.

Discussion

These data represent the first report of quantitative molecular and cellular correlations between total/universal and order-level gut microbial populations and GALT levels of immune activation in the duodenum of HIV-infected subjects. While the duodenal tissue and stool are located in distant locations in the GI tract, it is important to recognize that the microbiota identified in the stool are derived from the populations of bacteria from throughout the intestinal tract as intra-luminal contents shed communities by desquamation and mechanical motility. Notably, at higher-taxonomic levels (i.e. order-level), it is thought that the microbiota community structure is much more stable than lower-taxa levels (i.e. species) and therefore, the changes we observed were unlikely to be due to day to day variability as significant perturbations (such as acute disease or drugs) would be required to cause these kinds of dramatic shifts.²⁸⁻³⁰

This work confirms and extends the observations published by Gori *et al.*, who reported that the frequency of *Pseudomonas aeruginosa* in the stools of HIV-infected subjects was higher than in historical controls from the normal population.³¹ In this pilot study, the order Enterobacteriales, which contains a wide range of classically Gram-negative staining and pathogenic aerotolerant and facultative-anaerobic bacteria including *P. aeruginosa*, generally residing in small gut niches and producing strong TLR-4-stimulatory endotoxin-LPS was found in approximately 10-fold higher frequency in the HIV-positive subjects not on ART as compared to the control subjects ($p=0.099$). While the mechanisms of CD4⁺ T-cell depletion have been assumed to be multifactorial with accelerated immunosenescence as an important pathway, a contributing stimulus from pro-inflammatory Gram-negative gut bacteria has not previously been identified. However, several authors have suggested that increased gut permeability and plasma LPS levels are factors contributing to lymphocyte

apoptosis.³² Marchetti *et al.* have suggested that incomplete immune reconstitution is similarly causally related to the higher level of microbial rDNA translocation with sequences also specific to Enterobacteriaceae, a pro-inflammatory opportunistic family of gut bacteria within the Enterobacteriales order.³³

Our direct correlation of the quantitatively-dominant obligate-anaerobic order Bacteroidales (which also contain Gram-negative/LPS-containing species) with peripheral CD8⁺ T-cell activation is the first report of a relationship between gut luminal bacterial contents and systemic immune activation in HIV-infected subjects. It is interesting to note that Bacteroidetes is a dominant anaerobic large bowel organism, whereas Enterobacteriales is thought to be more dominant in the small bowel where facultative anaerobes and aerotolerant species reside. Our results also confirm and extend the work by Jiang *et al.*, who reported a correlation between systemic surrogate markers of bacterial translocation and immune activation.⁷ Although TLR-4 signaling by LPS has been implicated as the pathway for tissue and systemic immune activation, identification of the key species within the Bacteroidales order that are linked to systemic activation may facilitate alternate signal pathways of immune activation. While many species within the Bacteroidales order are commensals/mutualists participating in digestion/metabolism and produce weak TLR-4-stimulatory LPS, others are opportunistic pathogens containing several other pro-inflammatory TLR surface-antigens.

The inverse correlation observed between absolute bacterial numbers and tissue activation including both HIV-infected and control subjects suggest that this relationship represents a continuum of homeostatic factors influenced by the disease state. In HIV disease, the pro-inflammatory impact of a persistent systemic infection as well as bacterial antigen translocation likely amplifies the local tissue responses in the GI tract. These data are consistent with the large body of literature on gnotobiotic animal models which has demonstrated that the resident gut microbiota maintains baseline immune surveillance and health.³⁴ In germ-free animal models, sufficient repopulation of the intestinal microbiota is necessary to maintain physiologic intestinal inflammation. In a similar fashion, we observed in humans that the lowest levels of bacteria were observed in those with increased tissue level immune activation. Our observations cannot distinguish the directionality of the shifts in tissue activation/T-cell populations and the changes in gut microbiota populations. The experimental mouse model for addressing this question described by Finlay *et al.* may shed light on this question.³⁵ They demonstrated that the introduction of pathogenic Enterobacteriales species reduces total gut microbial density and, independently, experimentally-induced intestinal tissue inflammation promotes the specific overgrowth/bloom of pathogenic and non-pathogenic facultative-anaerobes (e.g. Enterobacteriaceae).³⁵ This work by Finlay and that of others has led to the hypothesis that the environmental state of gut inflammation increases the availability of nutrients to the microbes surviving the inflammatory event through the provision of rich oxygen radical exudative fluids via host phagocytic respiratory-bursts.³⁶ While these defenses may prevent systemic translocation in the host in the healthy state, they can provide pathogens with competitive growth advantages that co-regulate the resident microbiota and impede recovery after inflammatory events have resolved. Winter *et al.* have exquisitely reviewed these “blessings/curses” of gut inflammation as well as the mechanistic-investigations leading to those hypotheses.³⁷ Indeed, if the pathogenic changes observed in this pilot study are bidirectional and potentially self-propagated, corrective interventions will need to be directed at both the tissue and luminal compartments.

Although the focus of this pilot project was on gut microbial communities and the local tissue environment, the finding of a weak correlation between sCD14 as well as both CD4⁺ and CD8⁺ T-cell activation in the duodenal tissue is supportive of the potential systemic

effects of gut ecology. In this regard, our findings are consistent with the association between disruption of intestinal CD4⁺ T-cell homeostasis and systemic immune activation that was recently demonstrated by Gordon and colleagues.³⁸

McKenna *et al.* recently reported extensive sequencing analysis of 16S rDNA from multiple sites within the GI tract of rhesus macaques.³⁹ They observed that four acutely SIV-infected animals had similar bacterial populations compared to controls over the two months following infection, though individual animals in each group were noted to have significant co-morbid conditions including colitis at baseline, which dominated any differences between groups. These findings would be expected if chronic local immunodeficiency or systemic pro-inflammatory changes shift the gut ecology over time. They also reported that the populations of bacteria were distinct between humans and macaques, so it is uncertain at this time whether chronic HIV infection and SIV infection will result in parallel alterations in gut microbial communities.

In summary, the observed correlations between pro-inflammatory populations of bacteria in the gut of chronically infected HIV subjects and immunologic abnormalities may be due in part to a number of factors. The selective effect of persistent HIV replication⁴⁰ in the setting of an inflamed gut environment (primary site of early HIV pathogenesis) may perpetuate an inflammatory cycle⁴¹ weakening of mucosal barrier integrity, leading to whole community microbiota stimulation of underlying lymphoid tissue and microbial product translocation into periphery.⁴² Future studies of the correlations between bacterial translocation and extensive sequencing from both sites will aim to further define putative pathologic mechanisms that lead to the observed local and systemic immune activation and T-cell depletion.

Acknowledgments

The authors would like to thank Dr. Barbara Shacklett for her review and editing of the manuscript.

Collin L. Ellis received support from: The Richard A. and Nora Eccles Harrison Endowed Fund in Diabetes Research; the UC Davis T32 Predoctoral Clinical Research Training Program Scholar Award (The NIH-NCRR & NIH-Roadmap for Medical Research Grant Number UL1 RR024146); and the UC Davis Professors for the Future Program (Predoctoral Fellowship Award).

John C. Rutledge received support from: NIH NHLBI 55667

David M. Asmuth received support from: The National Center for Research Resources (NCRR), a component of the National Institutes of Health (NIH), and NIH Roadmap for Medical Research (Grant Number UL1 RR024146). The California HIV/AIDS Research Program of the University of California, Grant Number CH05-D-606

Statistical support for this publication was made possible by Grant Number UL1 RR024146 from the National Center for Research Resources (NCRR), a component of the National Institutes of Health (NIH), and NIH Roadmap for Medical Research. Its contents are solely the responsibility of the authors and do not necessarily represent the official view of NCRR or NIH. Information on Re-engineering the Clinical Research Enterprise can be obtained from <http://nihroadmap.nih.gov/clinicalresearch/overview-translational.asp>.

Reference List

1. Brenchley JM, Schacker TW, Ruff LE, et al. CD4⁺ T cell depletion during all stages of HIV disease occurs predominantly in the gastrointestinal tract. *J Exp Med.* 2004; 200:749–759. [PubMed: 15365096]
2. Wang X, Rasmussen T, Pahar B, et al. Massive infection and loss of CD4⁺ T cells occurs in the intestinal tract of neonatal rhesus macaques in acute SIV infection. *Blood.* 2007; 109:1174–1181. [PubMed: 17047153]

3. Mehandru S, Poles MA, Tenner-Racz K, et al. Primary HIV-1 infection is associated with preferential depletion of CD4⁺ T lymphocytes from effector sites in the gastrointestinal tract. *J Exp Med*. 2004; 200:761–770. [PubMed: 15365095]
4. Gautreaux MD, Deitch EA, Berg RD. T lymphocytes in host defense against bacterial translocation from the gastrointestinal tract. *Infect Immun*. 1994; 62:2874–2884. [PubMed: 7911786]
5. Gautreaux MD, Deitch EA, Berg RD. Bacterial translocation from the gastrointestinal tract to various segments of the mesenteric lymph node complex. *Infect Immun*. 1994; 62:2132–2134. [PubMed: 8168984]
6. Brenchley JM, Price DA, Schacker TW, et al. Microbial translocation is a cause of systemic immune activation in chronic HIV infection. *Nat Med*. 2006; 12:1365–1371. [PubMed: 17115046]
7. Jiang W, Lederman MM, Hunt P, et al. Plasma Levels of Bacterial DNA Correlate with Immune Activation and the Magnitude of Immune Restoration in Persons with Antiretroviral-Treated HIV Infection. *J Infect Dis*. 2009; 199:1177–1185. [PubMed: 19265479]
8. Giorgi JV, Detels R. T-cell subset alterations in HIV-infected homosexual men: NIAID Multicenter AIDS cohort study. *Clin Immunol Immunopathol*. 1989; 52:10–18. [PubMed: 2656013]
9. Deeks SG, Kitchen CM, Liu L, et al. Immune activation set point during early HIV infection predicts subsequent CD4⁺ T-cell changes independent of viral load. *Blood*. 2004; 104:942–947. [PubMed: 15117761]
10. Robbins GK, Spritzler JG, Chan ES, et al. Incomplete reconstitution of T cell subsets on combination antiretroviral therapy in the AIDS Clinical Trials Group protocol 384. *Clin Infect Dis*. 2009; 48:350–361. [PubMed: 19123865]
11. Kitchens RL, Thompson PA. Modulatory effects of sCD14 and LBP on LPS-host cell interactions. *J Endotoxin Res*. 2005; 11:225–229. [PubMed: 16176659]
12. Nockher WA, Bergmann L, Scherberich JE. Increased soluble CD14 serum levels and altered CD14 expression of peripheral blood monocytes in HIV-infected patients. *Clin Exp Immunol*. 1994; 98:369–374. [PubMed: 7527738]
13. Lien E, Aukrust P, Sundan A, Muller F, Froland SS, Espevik T. Elevated levels of serum-soluble CD14 in human immunodeficiency virus type 1 (HIV-1) infection: correlation to disease progression and clinical events. *Blood*. 1998; 92:2084–2092. [PubMed: 9731066]
14. Sandler NG, Wand H, Roque A, et al. Plasma Levels of Soluble CD14 Independently Predict Mortality in HIV Infection. *J Infect Dis*. 2011
15. Qin J, Li R, Raes J, et al. A human gut microbial gene catalogue established by metagenomic sequencing. *Nature*. 2010; 464:59–65. [PubMed: 20203603]
16. Vaarala O, Atkinson MA, Neu J. The "perfect storm" for type 1 diabetes: the complex interplay between intestinal microbiota, gut permeability, and mucosal immunity. *Diabetes*. 2008; 57:2555–2562. [PubMed: 18820210]
17. Vijay-Kumar M, Aitken JD, Carvalho FA, et al. Metabolic syndrome and altered gut microbiota in mice lacking Toll-like receptor 5. *Science*. 2010; 328:228–231. [PubMed: 20203013]
18. De La Serre CB, Ellis CL, Lee J, Hartman AL, Rutledge JC, Raybould HE. Propensity to high-fat diet-induced obesity in rats is associated with changes in the gut microbiota and gut inflammation. *Am J Physiol Gastrointest Liver Physiol*. 2010; 299:G440–G448. [PubMed: 20508158]
19. Garrett WS, Gallini CA, Yatsunenko T, et al. Enterobacteriaceae act in concert with the gut microbiota to induce spontaneous and maternally transmitted colitis. *Cell Host Microbe*. 2010; 8:292–300. [PubMed: 20833380]
20. Shacklett BL, Yang O, Hausner MA, et al. Optimization of methods to assess human mucosal T-cell responses to HIV infection. *Journal of Immunological Methods*. 2003; 279:17–31. [PubMed: 12969544]
21. Li Q, Duan L, Estes JD, et al. Peak SIV replication in resting memory CD4⁺ T cells depletes gut lamina propria CD4⁺ T cells. *Nature*. 2005; 434:1148–1152. [PubMed: 15793562]
22. Vaccari M, Boasso A, Ma ZM, et al. CD4⁺ T-cell loss and delayed expression of modulators of immune responses at mucosal sites of vaccinated macaques following SIV(mac251) infection. *Mucosal Immunol*. 2008; 1:497–507. [PubMed: 19079217]

23. Hartman AL, Lough DM, Barupal DK, et al. Human gut microbiome adopts an alternative state following small bowel transplantation. *Proc Natl Acad Sci U S A*. 2009; 106:17187–17192. [PubMed: 19805153]
24. Cole JR, Wang Q, Cardenas E, et al. The Ribosomal Database Project: improved alignments and new tools for rRNA analysis. *Nucleic Acids Res*. 2009; 37:D141–D145. [PubMed: 19004872]
25. Amann RI, Binder BJ, Olson RJ, Chisholm SW, Devereux R, Stahl DA. Combination of 16S rRNA-targeted oligonucleotide probes with flow cytometry for analyzing mixed microbial populations. *Appl Environ Microbiol*. 1990; 56:1919–1925. [PubMed: 2200342]
26. Rinttilä T, Kassinen A, Malinen E, Krogus L, Palva A. Development of an extensive set of 16S rDNA-targeted primers for quantification of pathogenic and indigenous bacteria in faecal samples by real-time PCR. *J Appl Microbiol*. 2004; 97:1166–1177. [PubMed: 15546407]
27. Castillo M, Martin-Orue SM, Manzanilla EG, Badiola I, Martin M, Gasa J. Quantification of total bacteria, enterobacteria and lactobacilli populations in pig digesta by real-time PCR. *Vet Microbiol*. 2006; 114:165–170. [PubMed: 16384658]
28. Vanhoutte T, Huys G, Brandt E, Swings J. Temporal stability analysis of the microbiota in human feces by denaturing gradient gel electrophoresis using universal and group-specific 16S rRNA gene primers. *FEMS Microbiol Ecol*. 2004; 48:437–446. [PubMed: 19712312]
29. Thompson CL, Hofer MJ, Campbell IL, Holmes AJ. Community dynamics in the mouse gut microbiota: a possible role for IRF9-regulated genes in community homeostasis. *PLoS ONE*. 2010; 5:e10335. [PubMed: 20428250]
30. Claesson MJ, Cusack S, O'Sullivan O, et al. Microbes and Health Sackler Colloquium: Composition, variability, and temporal stability of the intestinal microbiota of the elderly. *Proc Natl Acad Sci U S A*. 2010
31. Gori A, Tincati C, Rizzardini G, et al. Early impairment of gut function and gut flora supporting a role for alteration of gastrointestinal mucosa in human immunodeficiency virus pathogenesis. *J Clin Microbiol*. 2008; 46:757–758. [PubMed: 18094140]
32. Lackner AA, Mohan M, Veazey RS. The gastrointestinal tract and AIDS pathogenesis. *Gastroenterology*. 2009; 136:1965–1978. [PubMed: 19462506]
33. Marchetti G, Bellistri GM, Borghi E, et al. Microbial translocation is associated with sustained failure in CD4+ T-cell reconstitution in HIV-infected patients on long-term highly active antiretroviral therapy. *AIDS*. 2008; 22:2035–2038. [PubMed: 18784466]
34. Tlaskalova-Hogenova H, Stepankova R, Hudcovic T, et al. Commensal bacteria (normal microflora), mucosal immunity and chronic inflammatory and autoimmune diseases. *Immunol Lett*. 2004; 93:97–108. [PubMed: 15158604]
35. Lupp C, Robertson ML, Wickham ME, et al. Host-mediated inflammation disrupts the intestinal microbiota and promotes the overgrowth of Enterobacteriaceae. *Cell Host Microbe*. 2007; 2:119–129. [PubMed: 18005726]
36. Winter SE, Thiennimitr P, Winter MG, et al. Gut inflammation provides a respiratory electron acceptor for Salmonella. *Nature*. 2010; 467:426–429. [PubMed: 20864996]
37. Winter SE, Kestra AM, Tsois RM, Baumler AJ. The blessings and curses of intestinal inflammation. *Cell Host Microbe*. 2010; 8:36–43. [PubMed: 20638640]
38. Gordon SN, Cervasi B, Odorizzi P, et al. Disruption of intestinal CD4+ T cell homeostasis is a key marker of systemic CD4+ T cell activation in HIV-infected individuals. *J Immunol*. 2010; 185:5169–5179. [PubMed: 20889546]
39. McKenna P, Hoffmann C, Minkah N, et al. The macaque gut microbiome in health, lentiviral infection, and chronic enterocolitis. *PLoS Pathog*. 2008; 4:e20. [PubMed: 18248093]
40. Yukl SA, Gianella S, Sinclair E, et al. Differences in HIV burden and immune activation within the gut of HIV-positive patients receiving suppressive antiretroviral therapy. *J Infect Dis*. 2010; 202:1553–1561. [PubMed: 20939732]
41. Nixon DE, Landay AL. Biomarkers of immune dysfunction in HIV. *Curr Opin HIV AIDS*. 2010; 5:498–503. [PubMed: 20978393]
42. Estes JD, Harris LD, Klatt NR, et al. Damaged intestinal epithelial integrity linked to microbial translocation in pathogenic simian immunodeficiency virus infections. *PLoS Pathog*. 2010; 6

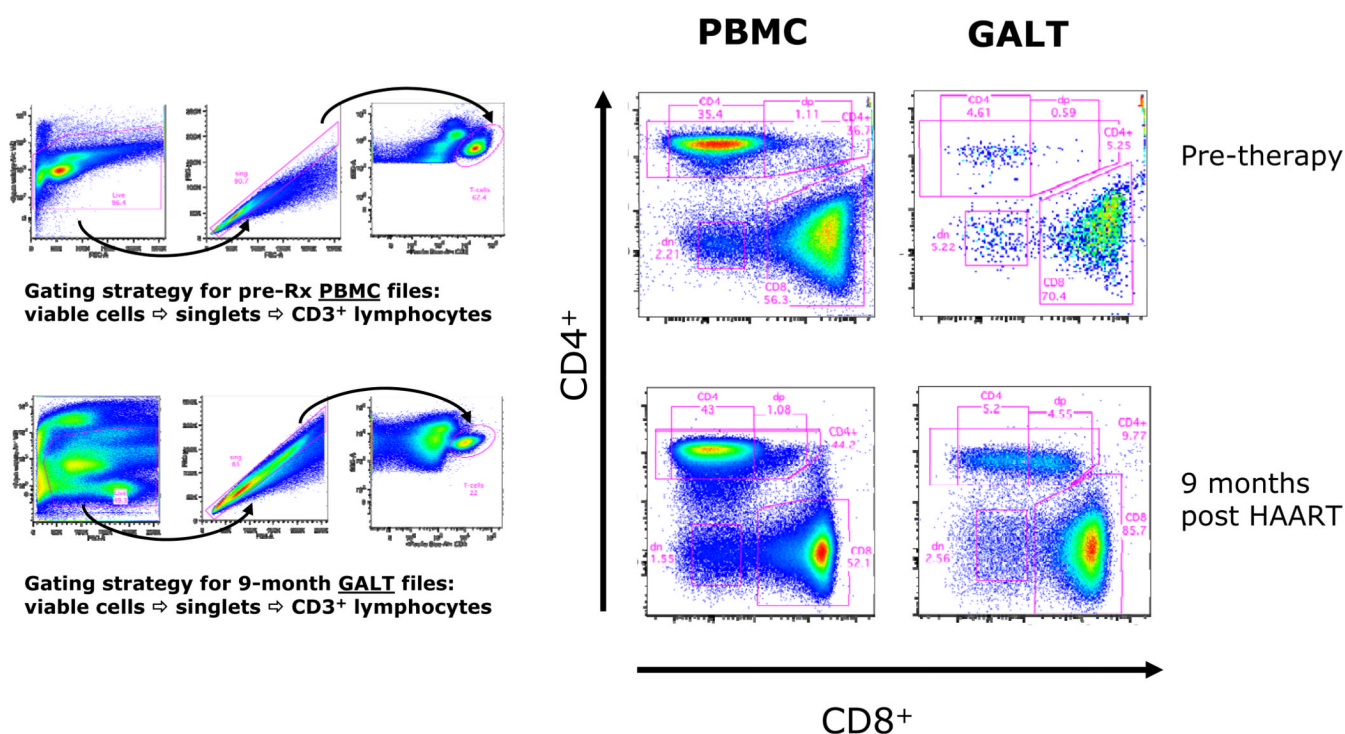


Figure 1. Gating Algorithm for Lymphocyte Analysis in PBMC and Duodenal Tissue
Gating strategy for all analysis first involved exclusion of dead cells as determined by viability dye exclusion staining followed by doublet discrimination gating for cells along the diagonal of the height and integrated area of the forward scatter signal. Gating was then carried forward of the CD3 positive population and CD4⁺ and CD8⁺ bivariate analysis.

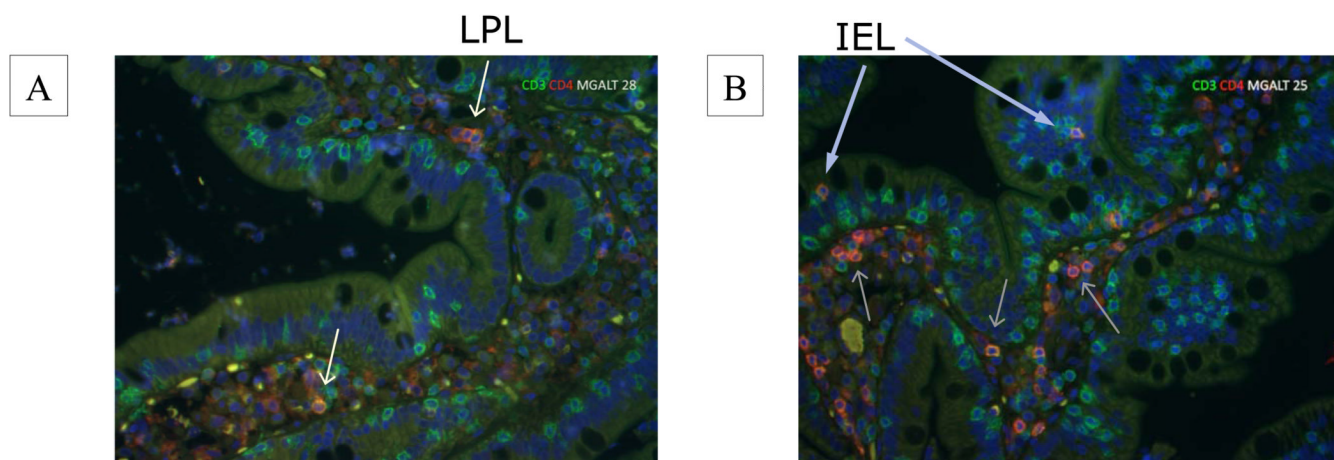


Figure 2. Immunohistochemistry of Duodenal Tissue Sections

IHC staining of duodenal tissue for double-positive intraepithelial (IEL) and lamina propria lymphocytes (LPL) for nuclei (DAPI-blue), CD3 (Alexa Fluor 488 - green) and CD4 (Alexa Fluor 568 - red).

No IEL (thick arrow) and few LPL (thin arrows) are seen in sections from HIV positive subjects (A) compared to control subjects (B). Mean duodenal CD3⁺/CD4⁺ count is 149 cell/mm² (± 44 cell/mm²) for pre-ART subjects by IHC; and 154 cell/mm² (± 25 cell/mm²) for post-ART subjects. All samples were read by a single observer blinded to the cohort assignment (Z-MM).

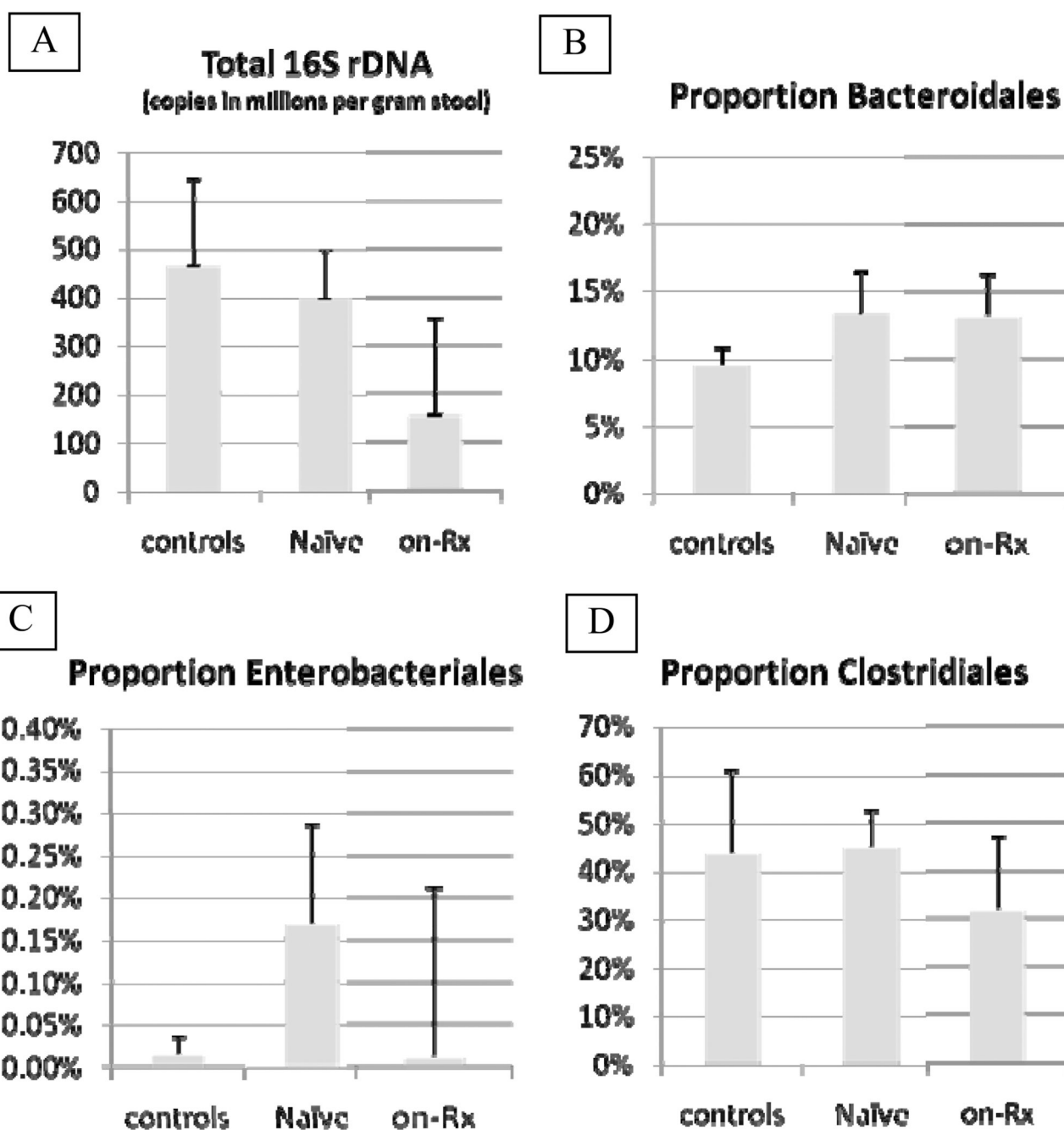


Figure 3. Total 16S rDNA and Proportion of Bacteria Orders in Stool by Treatment Group
 A: Total 16S rDNA in copies in millions of copies per gram stool wet weight. B – D: Triplicate qPCR mean-assay results for Bacteroidales, Enterobacteriales and Clostridiales orders expressed as a relative % of the panbacterial/total 16S rDNA load for that sample as described in the methods section. (error bars represent the standard error of the mean).

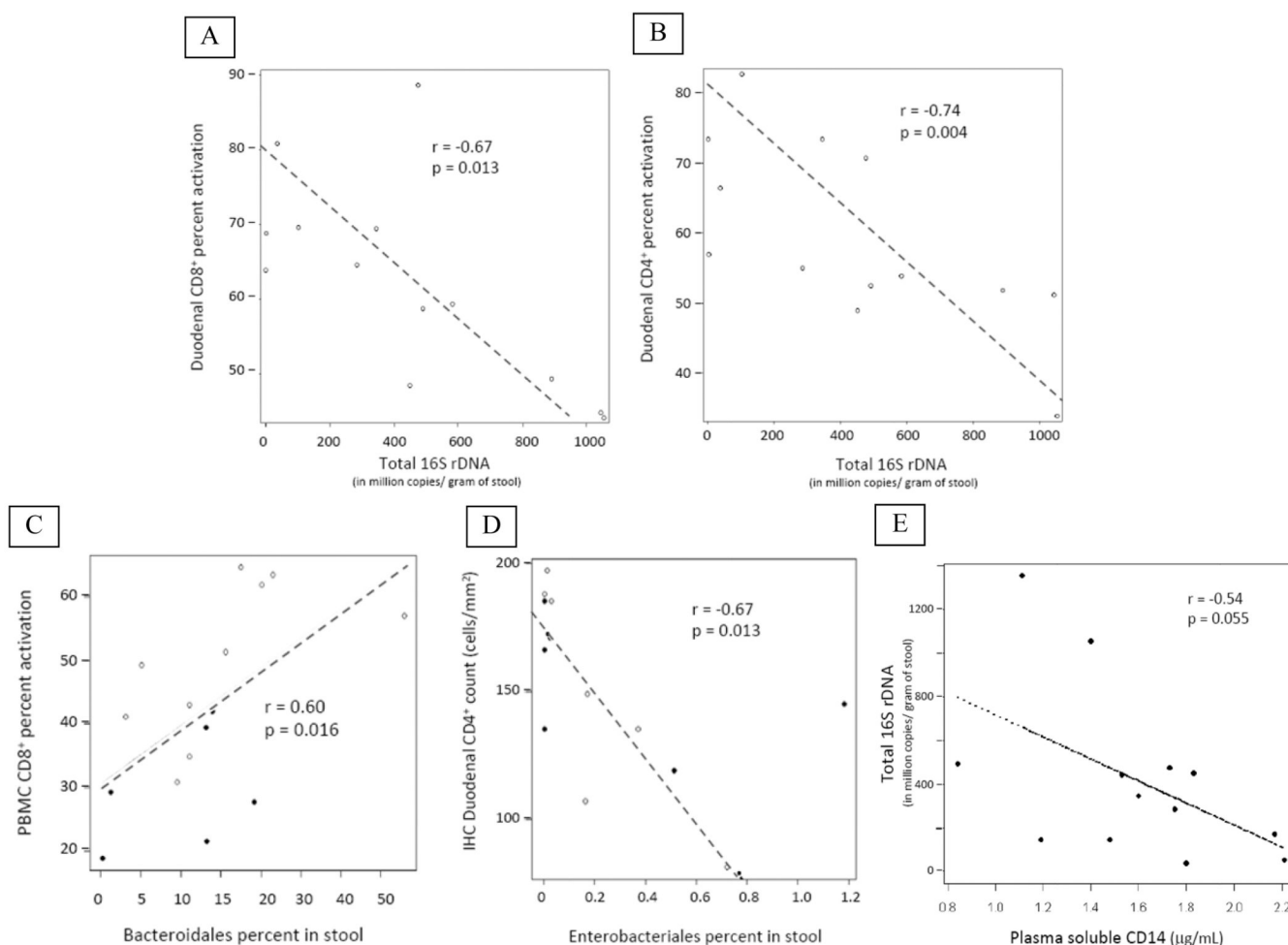


Figure 4. Correlations Between Gut Microbial Communities and Local and Systemic Immunologic Parameters

A and B: Correlation between Total 16S rDNA and tissue T-cell activation percentage. C: Correlation between Bacteroidales proportion in the stool and peripheral CD8⁺ T-cell activation levels. D: Correlation between Enterobacteriales proportion in the stool and CD4⁺ T-cell numbers in the corresponding lamina propria by IHC. E: Correlation between Plasma soluble CD14 in μg/mL and Total 16S rDNA. For C and D: Open circles – antiretroviral naïve subjects; solid circles – subjects after nine months of therapy

Table 1

Subject Demographics				
	normal control	ART Naïve	ART Experienced	all subjects
N	5	10	6	12
Male/Female	3/2	5/5	5/1	7/5
race/ethnicity *	1/1/0/2/1	3/6/1/0/0	0/5/1/0/0	3/8/1/0/0
Age	42.8±9.4 (43; 32,54)	41.7±9.0 (42; 26,56)	38.5±11.6 (37.5;26,51)	40.6±9.0 (40.5; 26,56)
pre-ART CD4	427.2±140 (433.5; 258, 651)		409.5±120.6 (391; 293, 593)	418.3±127.7 (433.5; 258, 651)
post-ART CD4	642.3±156.6 (657; 379,825)			

* African-American/Caucasian/Caucasian-Hispanic/Asian

12 subjects provided 16 paired stool-duodenal tissue/PBMC samples for inclusion in this pilot study. Four participants were studied both before and after 9 months of antiretroviral therapy.